J Polym Environ (2018) 26:2268–2280
DOI 10.1007/s10924-017-1121-3

ORIGINAL PAPER

Fabrication of Admicelled Natural Rubber by Polycaprolactone for Toughening Poly(lactic acid)

Warangkhana Phromma[1] · Rathanawan Magaraphan[1]

Published online: 9 October 2017

Abstract Natural rubber (NR) with polycaprolactone (PCL) core–shell (NR-ad-PCL), synthesized by admicellar polymerization, was acted as an impact modifier for poly(lactic acid) (PLA). PLA and NR-ad-PCL were melt-blended using a co-rotating twin screw extruder. The morphology of PLA/NR-ad-PCL blends showed good adhesion as smooth boundary around rubber particles and PLA matrix. Only 5 wt% of rubber phase, NR-ad-PCL was more effective than NR to enhance toughness and mechanical properties of PLA. The contents of the NR-ad-PCL were varied from 5, 10, 15 and 20 wt%. From thermal results, the incorporation of the NR-ad-PCL decreased the glass transition temperature and slightly increased degree of crystallinity of PLA. Mechanical properties of the PLA/NR-ad-PCL blends were investigated by dynamic mechanical analyser, pendulum impact tester and universal testing machine for tension and flexural properties. The increasing NR-ad-PCL contents led to decreasing Young's and storage moduli but increasing loss modulus. Impact strength and elongation at break of the PLA/NR-ad-PCL blends increased with increasing NR-ad-PCL content up to 15 wt% where the maximum impact strength was about three times higher than that of pure PLA and the elongation at break increased to 79%.

Keywords Admicellar polymerization · Mechanical properties · Natural rubber · Poly(lactic acid) · Toughness

✉ Rathanawan Magaraphan
Rathanawan.k@chula.ac.th

[1] Polymer Processing and Polymer Nanomaterials Research Unit, The Petroleum and Petrochemical College, Chulalongkorn University, Bangkok 10330, Thailand

Introduction

Poly(lactic acid) (PLA) is classified as a biodegradable polymer because it is made from agricultural products or renewable resources such as sugar cane, sugarbeets and other starch-rich products. PLA shows the good potential for many applications due to its good mechanical strength, excellent biodegradability, biocompatibility and easy processability. However, the limitation of this biodegradable polymer is brittleness, slow crystallization behavior, low softening temperature, and poor water and gas barrier properties [1–3]. Many modifications have been made to improve the mechanical properties of PLA, specifically its toughness, such as block-copolymerization [4] and blending with rubber [5, 6]. The toughness mechanism involves the cavitation of rubber particles and dilatational deformation of matrix. The plastic deformation of matrix blunts the crack tip which reduces the local stress concentration and allows the material to support higher load before failure occurs. Many research groups studied the toughening of PLA by blending with thermoplastic e.g. polyurethane (TPU) [7], linear low density polyethylene (LLDPE) [8] and poly(methyl methacrylate) (PMMA) [9]. Nonetheless, the biodegradable property is lost. Then the more interesting approach has been focused on blending with biodegradable polymers such as poly(butylene adipate-co-terephthalate) (PBAT), poly(butylene succinate) (PBS), polycaprolactone (PCL),and natural rubber [10].

Natural rubber (NR), owing to its high elasticity, high toughness and excellent elongation properties, has been used as an impact modifier for brittle plastics because the rubber particles can bridge the cracks resulting in preventing the crack growing. The increase in toughness of the polymer blends can be considered as the amount of elastic energy stored in the rubber particles and irreversibly dissipated [11]. Ishida et al. [12] studied the toughening

of PLA by melt blending with four types of rubbers: ethylene–propylene copolymer, ethylene–acrylic rubber, acrylonitrile–butadiene rubber (NBR), and isoprene rubber (IR). They found that IR showed high elongation and high ability to induce plastic deformation before break. Pongtanayut et al. [13] studied the blend of PLA/NR and PLA/ENR. The results showed that the elongation of PLA/NR at 10 wt% NR increased up to 25% as compared with that of pure PLA. The morphology of this blend observed plastic deformation with whitening zone and showed phase separation owing to mismatch of polarities between rubbers and PLA. Chumeka et al. [14] observed the mechanical properties of 90/10 PLA/NR blend and PLA/NR/poly(vinyl acetate) (PVAc) grafted NR at 90/5/5 wt%. The results showed that the morphology of the PLA/NR/PVac grafted NR showed shear yielding which corresponded to the highest elongation (16%) and impact strength (12 kJ/m^2). Thus, PVac acted as compatibilizer and promoted interfacial adhesion between PLA and NR phases. Sookprasert and Hinchiranan [15, 16] used the NR grafted PLA at 5 wt% as the compatibilizer for 80/20 PLA/NR blend. The morphology of blend showed partial miscibility with the impact strength 0.0625 kJ/m. Moreover, Ayutthaya and Poompradub [17] found that the highest elongation and impact strength were observed at 95% and 0.23 kJ/m, respectively in 100/15 PLA/NR blend by using ENR/PMMA co-compatibilizer at 3/1 phr. The possible reaction of ENR/PMMA was the epoxy groups in ENR reacted with the carboxyl groups in PLA and π–π interactions occurred between double bonds of NR and ENR. In addition, the carbonyl groups of PMMA could induce a dipole force with ester group of PLA. However, the increasing of PMMA decreased the elongation according to its high rigidity.

Ostafinska et al. [18] found the optimized composition of 80/20 PLA/PCL with good distribution of 0.6 μm PCL. The blend was partially miscible which attributed to decrease in modulus. The morphology of the PLA changed from crazing to shear yielding providing the highest impact strength (40 kJ/m^2). Kelnar et al. [19] observed the thermal and mechanical properties of 20/80 PLA/PCL blends. They found that the blends showed the decreasing of the glass transition temperature (T_g) and loss modulus as compared with that of pure PLA. Morover, the low molecular weight of PLA/PCL blends (1822 g/mol) decreased T_g to 31 °C and compressive modulus to 1 MPa. The strength of PLA/PCL blends decreased with increasing content of PCL as investigated by Felfel et al. [20]. Besides, the small content of PCL showed an improvement in toughness Chee et al. [21] further added a reactive compatibilizer, glycidyl methacrylate (GMA), at 3 wt% to a PLA/PCL blend at 85:15 ratio to enhance interfacial adhesion such that tensile strength was retained and elongation at break and impact strength were obviously enlarged. Luyt and Gasmi [22] found similar results that the blends of PLA/PCL at PCL 2–4 wt% reduced T_g due to the partially miscible.

In this work, a small amount of NR was blended with PLA in order to obtain good toughening properties; i.e. impact, tensile and flexural properties. Moreover, the new method to improve surface property of NR by admicellar polymerization was employed. This process creates ultrathin polymeric films with minimal chemical uses and can be applied on several substrate surfaces. This technique has four preparation steps as descripted by Pongprayoon et al. [23] and Bunsomsit et al. [24]. NR particles from natural rubber latex were used as micro-substrates for admicellar polymerization of ε-caprolactone monomer to yield NR-ad-PCL core–shell particles. Li et al. [25] showed that the rubber–acrylic (butyl acrylate–methyl methacrylate copolymer) core–shell particles dramatically increased toughness of PLA with increasing acrylic shell content up to 20.8 wt% which was the optimum content where the maximum toughness was obtained by the mechanisms of plastic deformation and rubber cavitations. Thus it was relevant to employ the surface modified NR with biodegradable core–shell structure, NR-ad-PCL, to improve mechanical properties of PLA. The NR-ad-PCL blended with PLA at various contents was prepared to compare their properties to those of the simple NR and PLA blends. Thermal, thermo-mechanical, morphological and mechanical properties of the PLA and NR-ad-PCL blends showed accordingly later that NR-ad-PCL core–shell particles could nicely provide good interfacial adhesion and thus allowing toughening mechanisms to enhance toughness of PLA effectively.

Materials and Methods

PLA (PLA2002D, D-content 4.25%, MFI 5.0–7.0 g/10 min at load 2.16 kg, 210 °C) was purchased from NatureWorks. NR was purchased from Rubber institute of Thailand. Ɛ-Caprolactone monomer and Tin(II) 2-ethylhexanoate ($SnOct_2$) were purchased from Sigma-Aldrich. Ethylene glycol was purchased from Poch SA. Cetyltrimethylammonium bromide (CTAB) was purchased from Merck. Epoxidize soybean oil (ESO) was purchased from Chemmin Company.

Preparation of Admicellar Polymerization of PCL Coated NR

Polymerization of ε-caprolactone monomer on NR latex particles was carried out by admicellar polymerization method. Dilute NR latex (5% w/w) was suspended in the CTAB surfactant (2800 μM) to obtain equilibrium concentration under basic condition. The mixture was stirred for 24 h to form bilayer of surfactant. After this period,

the ε-caprolactone monomer with 100 mM concentration was added into the mixture and stirred at 50 °C. After that, monomer:catalyst:initiator for 1000:1:100 were added to the solution of mixture to initiate polymerization of ε-caprolactone at 90 °C for 24 h [26]. After polymerization, the monomer conversion in admicelled rubber was determined based on the amount of monomer left in the reaction solution using UV–Visible spectrometer (Shimadzu, model UV-1800) at absorption band 230 nm. Then the NR-ad-PCL was washed by distilled water to remove the CTAB surfactant by centrifugation. The latex of NR-ad-PCL was used to determine the morphology and particle size from dynamic light scattering (DLS, Malvern model zetasizer nano series). Then, the NR-ad-PCL was dried in vacuum oven at 70 °C. The properties of NR-ad-PCL were showed in Table 1.

Preparation of the PLA Blends

50 g dry rubber content (DRC) of NR was precipitated by methanol and dried in vacuum oven at 70 °C for 24 h. The blend ratio of PLA and NR was 95:5 in weight percent. ESO used as a plasticizer was fixed at 4 parts per 100 of resin (phr) based on the total mass of PLA and NR. PLA, NR and ESO were fed in a co-rotating twin screw extruder (Lab-tech engineering) with L/D 40:1 and screw diameter of 20 mm. The speed of screw was operated at 30 rpm. The temperature profile started from 150 to 180 °C from the feed zone to the round die. Similarly, PLA, ESO and the NR-ad-PCL were prepared under the same preparation condition by varying the amount of NR-ad-PCL content at 5, 10, 15 and 20 wt%. The blended pellet was compressed by compression molding at 180 °C and 5 min for mechanical test.

Phase Morphology of NR-ad-PCL

The 5 g of cream NR from concentrated NR latex was re-dispersed in 100 g of distilled water and sonicated for 5 min. Similarly, from the prepared NR-ad-PCL emulsion, the 5 g sample was re-dispersed in 100 g of distilled water and sonicated for 5 min. TEM samples were obtained by dropping the dilute dispersion of NR or NR-ad-PCL on a 200 mesh copper grid and dried overnight. The dried sample of NR and the NR-ad-PCL was characterized by a transmission electron microscope (TEM, JEOL model JEM-1400), operated at an acceleration voltage of 100 kV. The size of the NR or NR-ad-PCL particle was calculated by averaging 20 particles from TEM images using a Java-based image processing and analysis program called Image J (developed at the National Institutes of Health).

Table 1 Properties of NR-ad-PCL

Properties of NR-ad-PCL	
The conversion of PCL (%)	43.5
The molecular weight of PCL (g/mol)	2625
The ratio of NR:PCL (wt%)	90.6:9.4
The glass transition of NR-ad-PCL (°C)	−52.3
The particle size of NR-ad-PCL (nm)[a]	1436 ± 70.7

[a]The particles size of NR was 262 ± 2.1 nm

Phase Morphology of the PLA Blends

The morphologies of the cryo-fractured surfaces from compression molding and impact fracture surfaces of pure PLA and the PLA blends were investigated by a scanning electron microscope (SEM, model Hitachi S-2500), with an accelerating voltage of 15 kV. Moreover, the surface morphology of the PLA/5 wt% NR blends from cryo-fractured surfaces and impact fracture surfaces was observed by a field-emission scanning electron microscope (FE-SEM, model Hitachi S-4800), with an accelerating voltage of 5 kV. The cross-sectional area was coated with platinum by a sputtering technique for 180 s prior to the observation. Additionally, the morphologies of the samples after tensile test of pure PLA and the PLA/15 wt% NR-ad-PCL blends were investigated by SEM, model Hitachi TM3000.

Thermal Analysis

The thermal properties of pure PLA and the PLA blends from a co-rotating twin screw extruder were characterized by differential scanning calorimeter (DSC, Mettler Toledo model DSC822e). In order to eliminate the thermal history, the samples were heated from 25 to 180 °C with a heating rate of 10 °C/min, and then cool from − 180 to 25 °C. For the last cycle, the samples were heated from 25 to 180 °C with a heating rate of 10 °C/min under nitrogen gas flow rate of 20 ml/min. The apparatus was calibrated with indium standard. The degree of crystallinity (χ_c) was calculated as seen in Eq. (1).

$$x_c = \frac{\Delta H_m - \Delta H_c}{W_f \times \Delta H_m^*} \times 100 \quad (1)$$

where ΔH_m was heat of fusion, ΔH_c was heat of crystallization, ΔH_m^* was 100% crystalline for PLLA (93.1 J/g) [3], 100% crystalline for PCL (139.3 J/g) [27] and W_f was the weight fraction of PLA component in the blends.

Dynamic Mechanical Analysis

The thermo-mechanical properties of pure PLA and the PLA blends wereperformed on a dynamic mechanical analyzer (DMA, model GABO-EPLEXOR 100N) using a constant frequency of 1 Hz and a temperature range from

− 80 to 120 °C. The measurement was carried out under tension mode with a static strain of 0.5% and a dynamic strain of 0.1%. The samples were prepared from compression molding. The dimensions of the test samples were 10 mm wide, 40 mm long and 3 mm thick.

Impact Test

Impact energy was tested by pendulum impact tester (Zwick model 5113) with the pendulum at 21.6 J, following ASTM D 256. The samples were prepared from compression molding. At least ten specimens of each sample were tested.

Tensile Test

Tensile properties were conducted using a universal testing machine (Instron, model 133R 4206), following ASTM D 882. The testing was employed with a crosshead load cell of 25 kN with a speed at 10 mm/min. The dimensions of the samples from compression molding were cut in a width 10 mm, a length 150 mm and a thickness 1 mm. At least ten specimens of each sample were tested. Tensile toughness was defined as the resistance to fracture of the materials under stress. Tensile toughness was determined by integrating the stress–strain curve in unit of Joule per cubic metre (J/m^3).

Flexural Test

Flexural properties: flexural strain at yield, flexural stress at 5%strain and flexural modulus of the PLA blends were measured with universal testing machine (Instron, model 133R 4206), following ASTM D 790. The size of the sample from compression molding was a width of 25 mm, a length of 80 mm, and a thickness 3 mm. The crosshead speed was 3 mm/min with crosshead load cell 5 kN and the support span length was 50 mm.

Results and Discussion

Phase Morphology of NR-ad-PCL

Surface morphology of the modified natural rubber with ε-caprolactone monomer obtained after reaction was observed by TEM as shown in the Fig. 1. From TEM image, the NR-ad-PCL exhibited core–shell structure. The dark circle was rubber particles and the outer layer as thin dark circle was PCL. The particle size of NR particles was ranged from 0.5 to 2 microns. The thickness of 3.2. Phase morphology of the PLA blends.

Figure 2 shows the SEM images of the cryo-fractured surfaces of all the PLA blends. The phase morphology of the NR-ad-PCL appeared as spherical domains (size < 2 microns) and the phase of PLA matrix was a smooth surface. Uniform distribution of the NR-ad-PCL particles

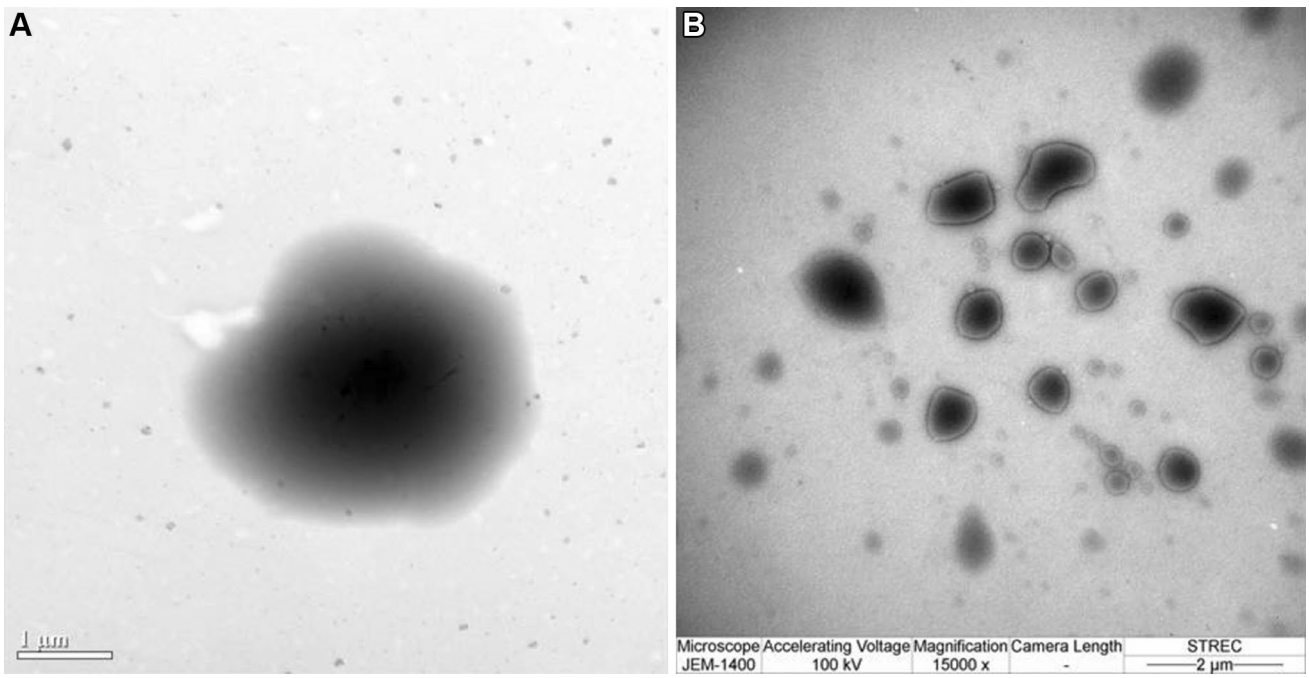

Fig. 1 TEM image of **a** green NR and **b** NR-ad-PCL

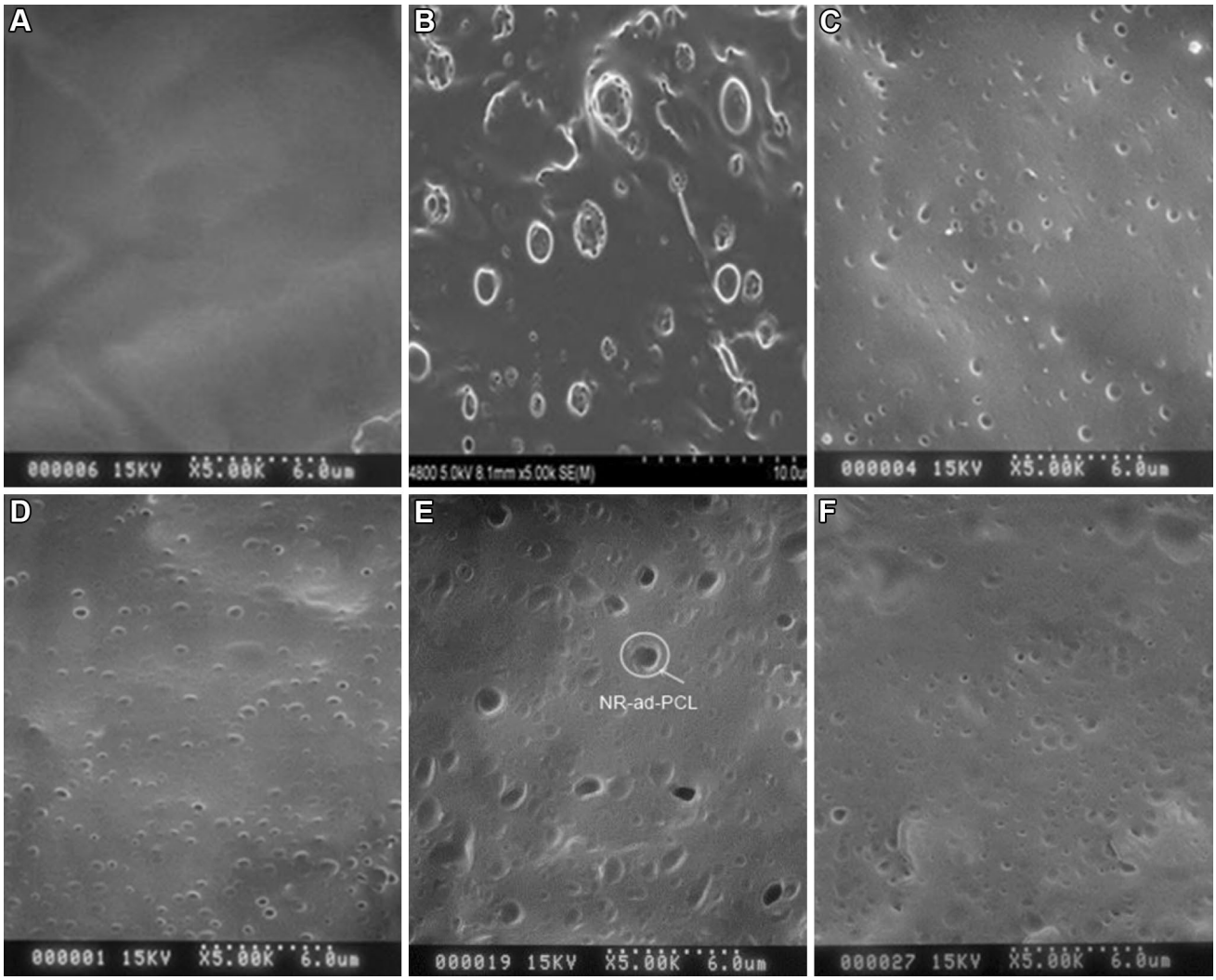

Fig. 2 SEM micrographs of cryo-fractured surfaces of **a** pure PLA, **b** PLA/5 wt% NR blends, **c** PLA/5 wt% NR-ad-PCL blends, **d** PLA/10 wt% NR-ad-PCL blends, **e** PLA/15 wt% NR-ad-PCL blends and **f** PLA/20 wt% NR-ad-PCL blends

in PLA matrix with homogeneous adhesion at the interface was observed. When the contents of the NR-ad-PCL increased, the large rubber domains were easily seen. In other words, agglomeration of the NR-ad-PCL brought about an increase in the size of its droplets and the distribution became less uniform. Moreover, there were rubber cavitations which typically occurred to allow toughening mechanism. The cavitation was mostly obvious in the blends with 15 wt% NR-ad-PCL. Comparably, the rubber domains in the PLA/5 wt% NR blends showed non uniform distribution of large aggregate domains with poor interface. So, the core–shell NR-ad-PCL successfully provided good adhesion and fine particle distribution to PLA matrix.

Thermal Properties of the PLA Blends

Table 2 shows the summary of thermal properties of pure PLA and its blends. Figure 3 shows the DSC thermograms of cooling (Fig. 3a) and second heating curves (Fig. 3b) of the PLA blends upon heating from 25 to 180 °C. Generally, there was no existence of any crystallization temperature (T_c) peaks during cooling in both pure PLA and the PLA blends (Fig. 3a) according to a very slow crystallization rate of PLA [28]. As compared to pure PLA, the glass transition temperature (T_g) (Fig. 3b) of the PLA/5 wt% NR blends and the PLA/5–20 wt% NR-ad-PCL blends decreased due to the incorporation of NR as an amorphous phase into the crystal phase of PLA matrix leading to increase flexibility.

Table 2 DSC results of PLA and the PLA blends with different NR-ad-PCL contents

Sample	T^g onset (°C)	T_{cc} onset (°C)	ΔH^c (J/g)	T^m peak (°C)	ΔH^m (J/g)	χ_c (%)
Pure PLA	56.97	106.09	25.83	150.77	27.59	1.89
Pure PCL	–	–	–	55.61	73.98	53.10
NR-ad-PCL	–	–	–	41.19 (onset)	0.83	–
5 wt% NR	54.70	107.99	20.21	150.95	20.52	0.35
5 wt% NR-ad-PCL	47.05	103.74	26.03	153.37	28.30	2.56
10 wt% NR-ad-PCL	47.26	101.72	19.40	153.44	21.67	2.71
15 wt% NR-ad-PCL	45.23	96.45	29.92	151.81	34.48	5.76
20 wt% NR-ad-PCL	43.35	93.74	28.68	150.89	31.84	4.24

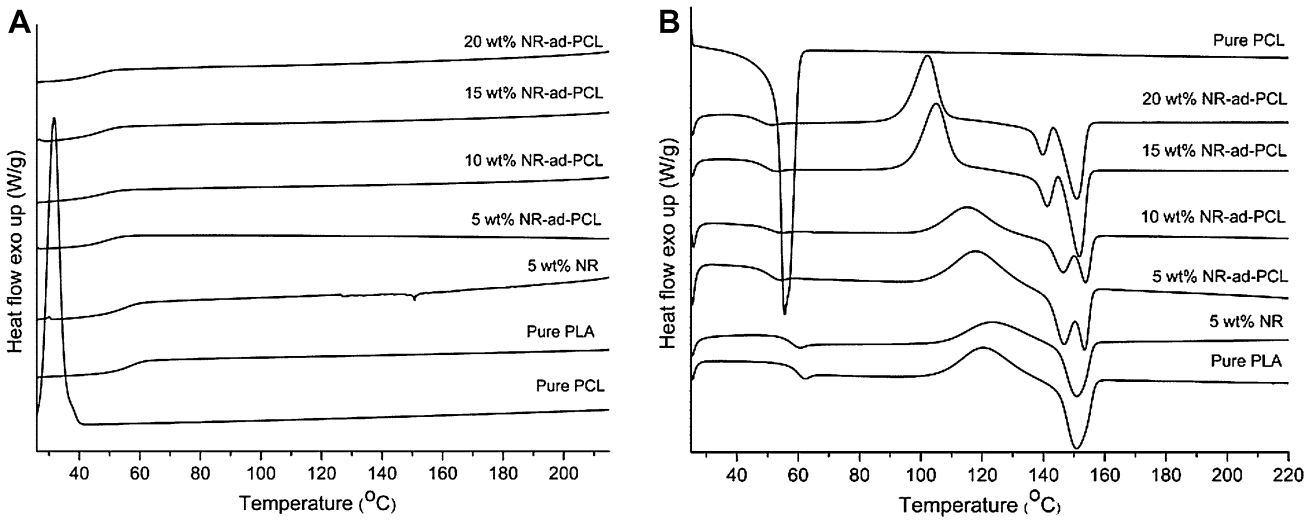

Fig. 3 Temperature dependence of heat flow with different contents of NR-ad-PCL **a** cooling and **b** second heat

Moreover, T_g of the PLA/5–20 wt% NR-ad-PCL blends were dropped much greater than that of the PLA/5 wt% NR blends. The PCL acted as a compatiblizer to promote the compatibility between PLA and NR phase. The solubility parameter of PLA and PCL closed to each other [29]. Therefore, T_g of PLA/NR-ad-PCL decreased as a result of PCL phase which promoted the adhesion between rubber and PLA (as seen in SEM results) providing the flexibility and mobility of PLA chains.

For the 5, 10, 15 and 20 wt% NR-ad-PCL, the onset cold crystallization temperatures (T_{cc}) occurred at lower temperature than that of the PLA/5 wt% NR blend (108 °C) and at decreasing temperature from 103.7 to 101.7, 96.5 and 93.7 °C, respectively. Similar results were reported by Bitinis et al. they suggested that the exothermic peak of T_{cc} of the PLA/NR blends resulted from NR enhancing crystallization ability of PLA or increasing the crystallization rate of PLA [10, 30]. Pure PLA had higher χ_c than that of the PLA/5 wt% NR blends. Nevertheless, χ_c of the PLA/5–20 wt% NR-ad-PCL blends was higher than that of pure PLA with the maximum at 15 wt% NR-ad-PCL suggesting that the NR-ad-PCL rather supported the crystallization of PLA as compared to pure NR. For the PLA/20 wt% NR-ad-PCL blends, χ_c decreased because the increasing of the amorphous phase of NR and thus the hindered formation of PLA crystals were more predominant [31]. Therefore NR-ad-PCL is more effective to facilitate cold crystallization and the degree of crystallinity of PLA than NR.

The pure PLA and the PLA/5 wt% NR blend showed only one melting peak at about 150.9 °C while PLA blends with NR-ad-PCL showed double melting peaks where the higher one was at 153.4 °C for 5 and 10 wt% NR-ad-PCL contents and became lower to 151.8 and 150.9 °C at lower NR-ad-PCL contents. There were two melting peaks due to the imperfect crystalline. Fukushima reported that the multi-peaks of endothermic PLA should link to the crystal structure reorganization upon melting. The imperfect crystalline generated at high cold crystallization temperature showed a high tendency to reorganize into a more ordered structure which was melted at high temperature [32]. PLA with 5–10 wt% NR-ad-PCL blends that showed rather high T_m due to less imperfect crystal was formed during cold crystallization providing reorganized to better perfect crystal and tightly packed crystal structure.

Thermo-Mechanical Properties of the PLA Blends

Table 3 shows the thermo-mechanical properties detected from DMA analysis. Figure 4 shows the loss factor (Fig. 4a), storage modulus (Fig. 4b) and tan δ (Fig. 4c) of pure PLA and its blends with NR and NR-ad-PCL at different contents, measured over the temperature range from − 80 to 120 °C. The loss modulus from low temperature to around room temperature revealed that the blends of the PLA/5 wt% NR blends had the lowest value informing that NR contributed most elasticity to the blends. For the PLA/5 wt% NR-ad-PCL blends, its loss modulus at room temperature was higher than that of PLA, PLA/5 wt% NR blends and rapidly increased as high as those of the PLA blends with 10 and 20 wt% NR-ad-PCL when temperature was closed to transition temperature. This infers that the NR-ad-PCL (containing low molecular weight PCL) contributes more chain mobility. The one with 15 wt% NR-ad-PCL had relatively low loss modulus around

Table 3 Thermo-mechanical properties from DMA analysis of PLA and its blends with different NR-ad-PCL contents

Sample	T_g at low temp (°C)	T_g at high temp (°C)	E′ @ 25 °C (MPa)	T_{cc} onset (°C)	Area under peak of PLA from tan δ
Pure PLA	–	67.8	2587	114.3	20.19
5 wt% NR	− 61.0	66.6	2260	97.5	18.57
5 wt% NR-ad-PCL	− 60.2	67.6	2190	98.4	18.65
10 wt% NR-ad-PCL	− 70.4	65.8	1751	92.2	19.79
15 wt% NR-ad-PCL	− 67.6	63.4	1713	92.6	22.20
20 wt% NR-ad-PCL	− 69.2	64.0	1241	93.6	19.88

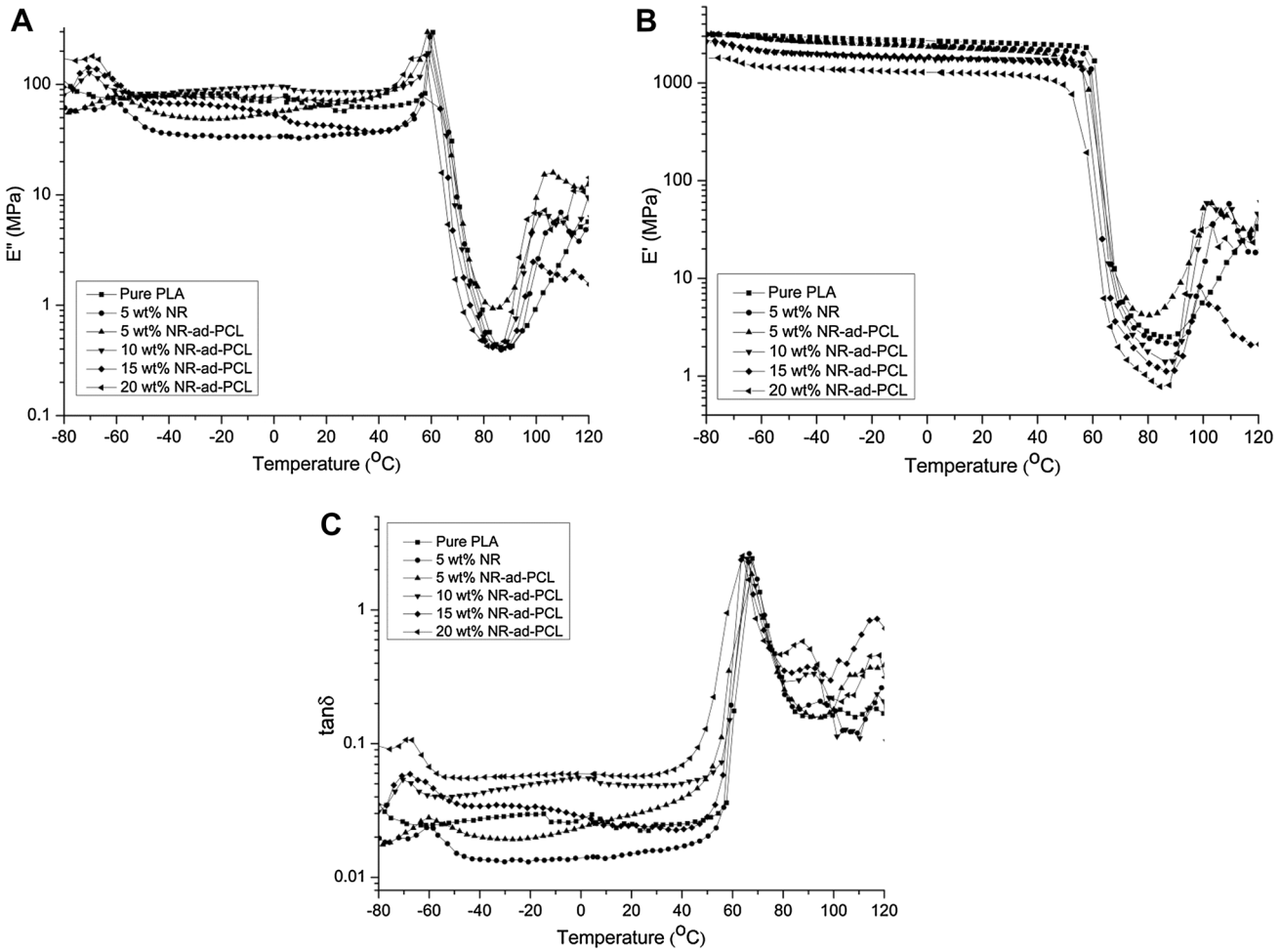

Fig. 4 DMA analysis of **a** loss modulus, **b** storage modulus, and **c** tan δ of pure PLA and the PLA blends with different contents of NR-ad-PCL

room temperature probably due to proper condition for PCL crystallization to suppress chain motion. Considering the storage modulus (Fig. 4b), PLA and its blends fell in three steps; the first was between −70 and −40 °C corresponding to glass transition of rubber, the second was between −40 and 70 °C where the storage moduli were rather steady and significantly decreased or softened near the glass transition of PLA, and the last step was between 70 and 120 °C where the storage modulus slightly increased with the corresponding T_{cc} of PLA [33]. The storage modulus of pure PLA at 25 °C was 2587 MPa and the storage modulus decreased when NR and the NR-ad-PCL were incorporated. As expected, NR decreased the storage modulus of PLA due to increasing the elastic phase [34]. The storage modulus of the PLA/5–20 wt% NR-ad-PCL blends was lower than that of the PLA/5 wt% NR blends. The results suggested that the NR-ad-PCL made the blends with PLA become soften and enhance chain mobility so the blends with high contents (15–20 wt%) of the NR-ad-PCL showed significantly decreasing in modulus, see Table 2. The onset of softening point of PLA occurred at lower temperature with increasing the NR-ad-PCL contents. In addition, the storage modulus exhibited the large drop to the minimum of < 1 MPa with increasing contents of the NR-ad-PCL, particularly 20 wt% NR-ad-PCL, due to the melted PCL. For above 90 °C, the storage moduli of all the PLA blends increased and higher than that of pure PLA because of cold crystallization of PLA. An increase in the chain mobility took place at high temperature, it thus favored the crystallization process [35]. At 100 °C, the storage moduli of the PLA blends were developed to higher than that of pure PLA, especially the one with 10 wt% NR-ad-PCL showing the storage modulus up to 58 MPa as compared to 7 MPa for pure PLA. It should be noted that the PLA/5 wt% NR-ad-PCL blends revealed the highest developed storage modulus among all samples at high temperature. These results corresponded to DSC thermal results that showed high melting temperatures of PLA/5 and 10 wt% NR-ad-PCL blends suggesting their good perfect crystal were formed.

The tan δ of the PLA blends showed two peaks corresponding to T_g at lower temperature resulted from NR or NR-ad-PCL phase, whereas T_g at higher temperature, resulted from PLA phase. T_g of pure PLA was 67.8 °C. When the contents of the NR-ad-PCL increased, T_g of PLA shifted to lower temperature suggesting their good compatibility. Thus, PLA and NR-ad-PCL formed a partially miscibility.

Impact Strength of the PLA Blends

As seen in Fig. 5 (see also Table 4), the impact strength of the PLA/5 wt% NR blends (9.80 kJ/m^2) was higher than that of pure PLA (6.45 kJ/m^2) due to energy dissipation

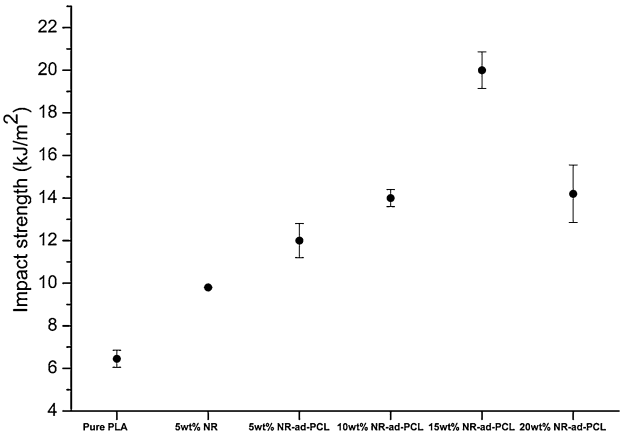

Fig. 5 Impact strength of PLA and its blends with different NR-ad-PCL contents

contributing from NR elastic phase [31]. However, the blends with 5 wt% NR-ad-PCL had its impact strength increasing to 12.55 kJ/m^2, larger than the blends with 5 wt% NR. Moreover, the impact strength increased further with increasing the NR-ad-PCL contents up to the maximum in the PLA/15 wt% NR-ad-PCL blends (20 kJ/m^2), about three times more than that of pure PLA. Further increasing the NR-ad-PCL content to 20 wt% brought about the decrease in impact strength (14 kJ/m^2) which corresponded to the lowering in its modulus and the presence of large agglomeration, Fig. 4f. The effectiveness of rubber toughened plastics was controlled by several factors, such as type and blend ratio of rubber, size and shape of the rubber particles, and the interfacial adhesion between rubber particles and matrix [12, 36]. The enhancement of the impact strength of PLA resulted from good interfacial adhesion, distribution, and dispersion of fine the NR-ad-PCL particles despite that thin PCL layer content was about 9 wt%. The NR-ad-PCL phase was helpful to absorb, dissipate the crack energy, and prevent the abrupt breaking of the sample [37]. At low content of NR-ad-PCL, the rubber particle is small while its bulk modulus is rather high; the energy used to cavitate rubber is thus higher than when particle is big. The rubber particles become larger (easier to cavitate) at high NR-ad-PCL content but the bulk modulus becomes lower such that the matrix yielding can occurred easier allowing more energy absorbed [38]. The bigger size of the NR-ad-PCL was observed in the PLA/20 wt% NR-ad-PCL blends that caused local stress concentration in broader region than the other blends, resulting in fast fracture progress, and therefore the impact strength became lower than the PLA/15 wt% NR-ad-PCL blends [39].

The impact fracture morphology was shown in Fig. 6 where the addition of the NR-ad-PCL allowed rubber cavitation with intensive matrix yielding to form fibrils. The

Table 4 Mechanical properties and impact strength of pure PLA and its blends with different NR-ad-PCL contents

Sample	Young modulus (MPa)	Tensile strength at yield (MPa)	Tensile strength at break (MPa)	Elongation at break (%)	Izod testing (kJ/m^2)	Tensile toughness (J/m^3) $\times 10^4$
Pure PLA	1972.14 ± 6.60	51.64 ± 1.06	49.18 ± 0.69	6.13 ± 0.21	6.45 ± 0.40	173.75
5 wt% NR	1776.41 ± 4.70	38.98 ± 0.44	16.06 ± 0.59	5.16 ± 0.40	9.80 ± 0.01	155.23
5 wt% NR-ad-PCL	1334.36 ± 13.87	45.83 ± 1.04	35.69 ± 3.28	7.22 ± 0.93	12.55 ± 0.80	220.95
10 wt% NR-ad-PCL	1169.64 ± 0.14	30.82 ± 0.89	16.61 ± 3.92	35.31 ± 5.35	14.83 ± 0.46	821.53
15 wt% NR-ad-PCL	1134.25 ± 7.66	29.98 ± 1.05	21.87 ± 0.15	79.44 ± 1.34	20.00 ± 0.86	1752.30
20 wt% NR-ad-PCL	1137.52 ± 12.72	23.75 ± 1.32	17.22 ± 0.71	15.52 ± 1.84	14.26 ± 1.35	322.21

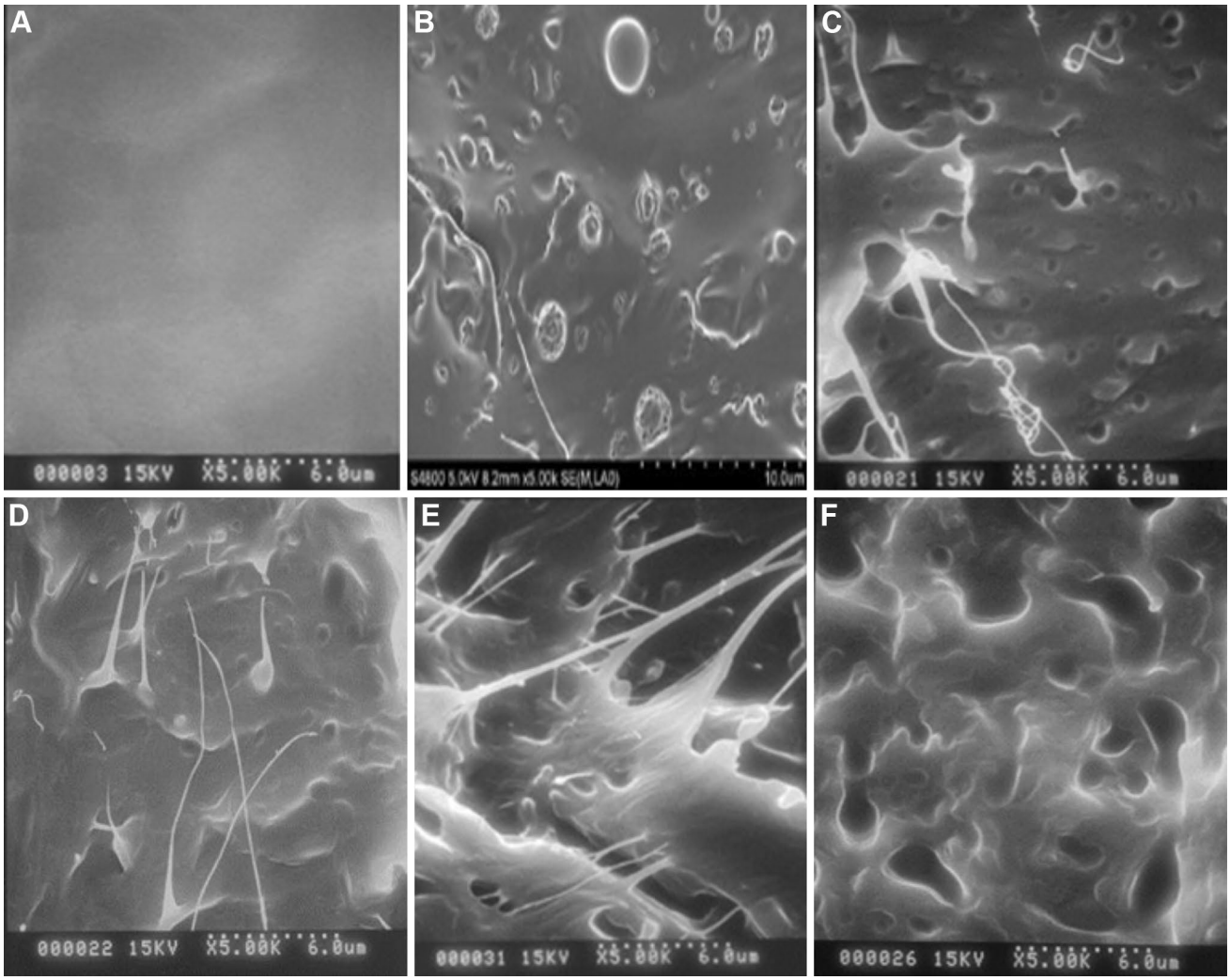

Fig. 6 SEM micrographs of impact fractured surfaces of **a** pure PLA, **b** PLA/5 wt% NR blends, **c** PLA/5 wt% NR-ad-PCL blends, **d** PLA/10 wt% NR-ad-PCL blends, **e** PLA/15 wt% NR-ad-PCL blends and **f** PLA/20 wt% NR-ad-PCL blends

fibrillation absorbed fracture energy and prevented the propagation of the crack [40]. At 5 wt% NR-ad-PCL, rubber cavitation was dominant and small number of matrix yielding; however, the matrix yielding became intensive with increasing the NR-ad-PCL content. The deformation causing extensive energy dissipation was most severe in the PLA/15 wt% NR-ad-PCL blends, where the maximum impact strength was achieved. When rubber cavitation was

initiated, the interfacial adhesion was typically stronger than the matrix yield stress so that the tri-axial stress field was relieved and transformed to induce shear yielding of the matrix [41]. The fibrillation occurred around the rubber particles inferred the large deformation associated with high energy absorption. Using 20 wt% NR-ad-PCL lowered the modulus and yield strength so that the failure mechanism was altered to rubber cavitation and debonding of the large rubber domains with some initiated yielding but none of fibrillation; i.e. crack propagating without large deformation of matrix. For comparison, the PLA/5 wt% NR blends showed limited matrix yielding.

The previous work of Li et al. showed impact strength improvement about five times for PLA blended with the synthesized rubber core–shell (polybutyl acrylate-co-methyl methacrylate, having PMMA shell content 18 wt%) of 20 wt% [25]. Besides good compatibility, the large improvement contributed from the high modulus of their synthesized core–shell particles. In our case, the biodegradable NR-ad-PCL core–shell was rather soft (much softer than PLA) and PCL was not as strong as PMMA so the toughening effect was limited at high loading as the modulus of the blends was decreased. Moreover, PCL shell was relatively thin due to its small content (9 wt%) but surprisingly, as preparing by admicellar polymerization, it was effective enough to provide good interfacial adhesion and thus could obviously improve toughness at low loading content e.g. twice at 5 wt% and three times (maximum) at 15 wt%.

Mechanical Properties of the PLA Blends

The mechanical properties were related to the miscibility of the polymer blend, the dispersed size and interfacial adhesion between the phases. Pure PLA was rigid and brittle polymer with low elongation at break of approximate 6%. The tensile results of PLA and its blends were shown in Table 4 and Fig. 7. As compared with those of pure PLA, the PLA blends exhibited low Young's modulus, yield strength and tensile strength at break, while the elongation at break of all blend samples was high. Yield strength and tensile strength at break of the PLA blends decreased with increasing the NR-ad-PCL contents. In general, the addition of a soft segment of rubber into a hard segment of PLA causes a decrease in the modulus and the strength of the blends.

Tensile properties of the PLA/5 wt% NR blends were obviously poorer than those of the PLA/5 wt% NR-ad-PCL blends suggesting the effect of good interfacial adhesion to bring about high yield strength, tensile strength and elongation at break but not the modulus due to the NR-ad-PCL enhancing chain mobility (high loss modulus). Increasing the NR-ad-PCL contents in the blends resulted in the moderate tensile strength. The good interfacial adhesion contributed to maintain high modulus, elongation at break

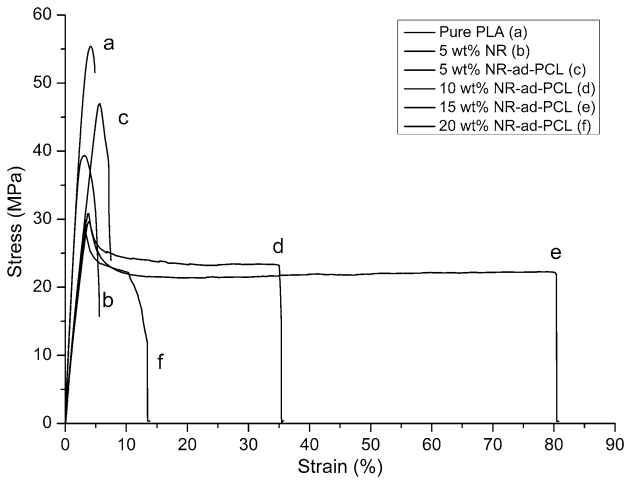

Fig. 7 Stress–strain curves of PLA and its blends with different NR-ad-PCL contents

and also toughness which could not obtain from simple the PLA/NR blends [13]. Figure 7 shows stress–strain curves of pure PLA and PLA blends. Pure PLA showed brittle properties with no necking owing to less plastic deformation as a result, the strain hardening was not observed. The yield stress of PLA/NR-ad-PCL blends decreased with the addition of NR-ad-PCL, and large plastic deformation (Fig. 9b) accompanying the necking was possible. This result suggested that NR behaved as a stress concentrator and the debonding in the initial stage of stretching which occurred at the particle–matrix interface as a result, the formation of a yield point at which stable plastic deformation took place [10]. The addition of the NR-ad-PCL into PLA matrix changed the brittle property of PLA to ductile property as observed from the maximum elongation at break (79%) and tensile toughness (1752.30 $J/m^3 \times 10^4$) of the PLA/15 wt% NR-ad-PCL blends. The increment of elongation at break was achieved to 120%, corresponding to the highest impact strength of the PLA/15 wt% NR-ad-PCL blends. Furthermore, the elongation at break of the PLA/20 wt% NR-ad-PCL blends decreased due to the agglomeration of the rubber particles larger than 2.4 μm as found in Fig. 6f. It was consistent with Chumeka et al. [14] and they suggested that the blends of PLA/NR showed lower tensile properties and impact strength because of the diameter larger than 2.1 μm. The decreasing in mechanical properties of the blends related to the decrease of modulus and yield stress with increasing rubber content. When the blends were a low modulus and low yield stress, the stress could not be transferred far from the crack corresponding to the crack propagation without a large deformation of matrix [38]. Therefore, the rubber particle size increased with increasing NR concentration, leading to a reduction in tensile properties.

Figure 8 shows the appearance of the samples after tensile test. All the PLA blends showed stress whitening when compared with pure PLA. The stress whitening was a consequence of cavity and crazes. This phenomenon was the combination of micromechanisms such as microcracks, microvoids, and stretched fibrils [42]. The extent of stress whitening of the PLA/5 wt% NR blends was much smaller than that of the PLA/5 wt% NR-ad-PCL blends. All PLA/NR-ad-PCL blends showed long stress whitening with high elongation with the most intensive in the PLA/15 wt% NR-ad-PCL blends. Figure 9a, b show the fractured surfaces after tensile test of pure PLA and the PLA/15 wt% NR-ad-PCL blends (as a representative of the PLA blends). Pure PLA showed the smooth fracture surface that meant brittle fracture. After addition the NR-ad-PCL into PLA matrix (Fig. 9b), the surface was changed to rough surface. The morphology exhibited cavitation and shear yielding where the arrow pointed. The cavitation of rubber particles played an important role in the toughening effect which released triaxial stresses surrounding cavitated particles to dissipate energy and giving more shear yielding [40, 43, 44]. Furthermore, fibrillar structure was detected, which tended to bridge and retard the propagation of the voids. The fibrillation was regarded as an energy adsorption domain.

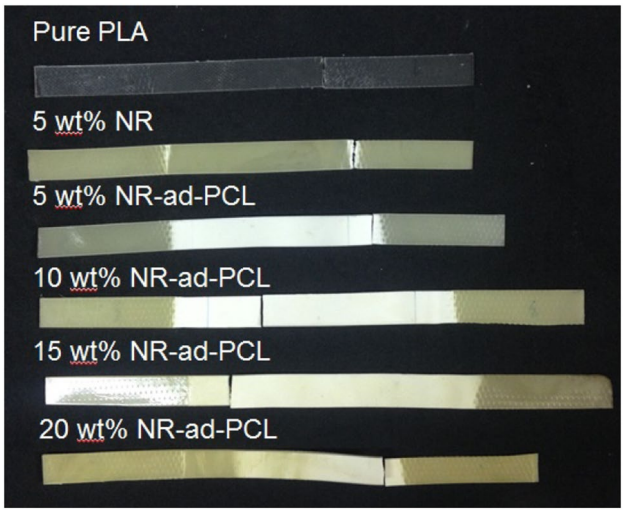

Fig. 8 Tensile specimens after testing of PLA and its blends

Flexural properties of the PLA blends

Flexural strength, flexural strength at 5%strain, flexural modulus a nd flexural strain of PLA and its blends were summarized in Table 5. It should be noted that only PLA sample was broken entirely but not others. This suggests that the brittle PLA was turned to a rather ductile material by adding rubber. The flexural strength at yield, flexural strength at 5%strain and the flexural modulus of pure brittle PLA were higher than that of the PLA/5 wt% NR blends which was higher than the PLA/5 wt% NR-ad-PCL blends. The flexural strength and flexural modulus of the PLA/5–20 wt% NR-ad-PCL blends decreased with increase the contents of the NR-ad-PCL. The un-entirely broken suggests good interfacial adhesion between PLA and NR or NR-ad-PCL. Similar to tensile properties, the reduction in flexural properties of the PLA/NR-ad-PCL blends was explained by the decrease in bulk modulus of the blends with increasing content of NR-ad-PCL which is softer and less elastic than NR.

It should be emphasized here that the NR particles covered by thin PCL layer (small content) produced from admicellar polymerization, provided good compatibility

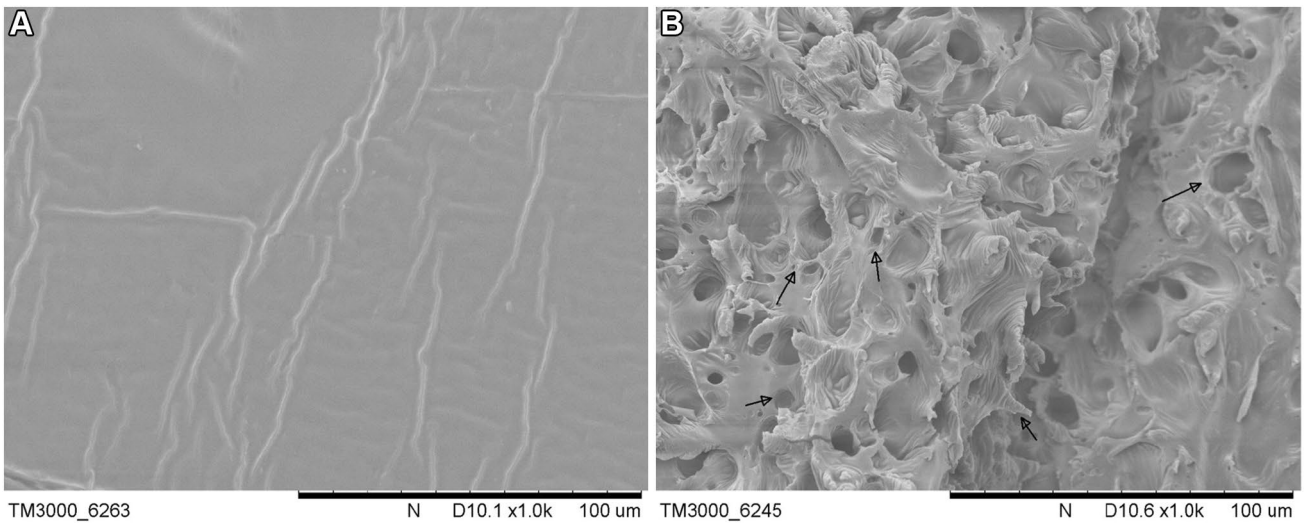

Fig. 9 SEM micrographs of sample after tensile testing **a** pure PLA and **b** PLA/15 wt% NR-ad-PCL blends

Table 5 Flexural test of pure PLA and its blends with different NR-ad-PCL contents

Sample	Flexural strength at yield (MPa)	Flexural strength at 5% strain (MPa)	Flexural modulus (at 1%) (MPa)	Flexural strain at yield (%)
Pure PLA	89.95 ± 0.21	83.67 ± 4.15	3150 ± 14.14	4.11 ± 0.01
5 wt% NR[a]	60.00 ± 0.42	53.45 ± 0.77	2310 ± 51.96	2.99 ± 0.01
5 wt% NR-ad-PCL[a]	55.33 ± 0.51	49.50 ± 0.42	2365 ± 63.63	3.18 ± 0.02
10 wt% NR-ad-PCL[a]	42.50 ± 0.42	37.75 ± 0.07	1903 ± 178.97	2.95 ± 0.01
15 wt% NR-ad-PCL[a]	40.00 ± 0.28	35.13 ± 1.15	1850 ± 42.42	2.66 ± 0.01
20 wt% NR-ad-PCL[a]	30.50 ± 1.27	26.40 ± 0.42	1465 ± 49.49	2.48 ± 0.03

[a]The test stopped before sample broke

between PLA and NR and resulted in uniform distribution of small size rubber particles. Considering from overall mechanical properties, the NR-ad-PCL even only small content 5 wt% was effectively contributed to improve toughness and mechanical properties of PLA although the PLA/15 wt% NR-ad-PCL blends showed the highest impact strength (about three times) and elongation at break (> 10 times).

Conclusion

It was clearly showed that the novel biodegradable core–shell particles, NR-ad-PCL, prepared admicellar polymerization could be used successfully to improve toughness of PLA. In comparison to PLA/NR, only 5 wt% of rubber phase, PLA/NR-ad-PCL blends showed uniform distribution of fine rubber particles in PLA matrix with good interfacial adhesion and possessed the superior toughening (impact, tensile, and flexural) properties. By increasing NR-ad-PCL content (5–20 wt%) in the PLA blends, the morphology still showed the good distribution of the NR-ad-PCL particles (of larger size) and smooth interfacial adhesion between PLA and the NR-ad-PCL phases. Compatibility between PLA and NR was improved by using NR-ad-PCL core–shell as evident from the shifting of T_g of PLA. Moreover, the NR-ad-PCL affected to decrease T_g, accelerate cold crystallization at lower temperature and increase χ_c of PLA. At small content of NR-ad-PCL, it caused less imperfect crystal (formed by cold crystallization) that readily transformed to good perfect crystal of high melting temperature as evident by DMA and DSC results. The storage modulus of the PLA blends decreased while the loss modulus increased suggesting more chain mobility with increasing the NR-ad-PCL contents. The toughness of the PLA/NR-ad-PCL blends was found in accordance to the decrease in T_g and bulk mod ulus. The highest impact strength (20 kJ/m^2) and elongation at break (79%) were obtained at 15 wt% NR-ad-PCL. The toughening mechanism was clearly seen by rubber cavitation and large deformation (fibrillation) of matrix around rubber domains.

Acknowledgements This work was granted by Thailand Research Fund through The Royal Golden Jubilee, Ph.D. Program (PHD/0044/2553). The Petroleum and Petrochemical College, Chulalongkorn University for their knowledge and assistance, including providing the equipment used in this research.

References

1. Yu L, Dean K, Li L (2006) Prog Polym Sci 31:576–602
2. Fortunati E, Armentano I, Zhou Q, Puglia D, Terenzi A, Berglund LA, Kenny JM (2012) Polym Degrad Stab 97:2027–2036
3. Lim LT, Auras R, Rubino M (2008) Prog Polym Sci 33:820–852
4. Rathi S, Chen X, Coughlin EB, Hsu SL, Golub CS, Tzivanis MJ (2011) Polymer 52:4184–4188
5. Grijpma DW, Van Hofslot RDA, Supèr H, Nijenhuis AJ, Pennings AJ (1994) Polym Eng Sci 34:1674–1684
6. Jaratrotkamjorn R, Khaokong C, Tanrattanakul V (2012) J Appl Polym Sci 124:5027–5036
7. Hong H, Wei J, Yuan Y, Chen F-P, Wang J, Qu X, Liu C-S (2011) J Appl Polym Sci 121:855–861
8. Anderson KS, Lim SH, Hillmyer MA (2003) J Appl Polym Sci 89:3757–3768
9. Choochottiros C, Chin I-J (2013) Eur Polym J 49:957–966
10. Bitinis N, Verdejo R, Cassagnau P, Lopez-Manchado MA (2011) Mater Chem Phys 129:823–831
11. Borggreve RJM, Gaymans RJ, Schuijer J (1989) Polymer 30:71–77
12. Ishida S, Nagasaki R, Chino K, Dong T, Inoue Y (2009) J Appl Polym Sci 113:558–566
13. Pongtanayut K, Thongpin C, Santawitee O (2013) Energy Procedia 34:888–897
14. Chumeka W, Tanrattanakul V, Pilard J-F, Pasetto P (2013) J Polym Environ 21:450–460
15. Sookprasert P, Hinchiranan N (2015) Macromol Symp 354:125–130
16. Sookprasert P, Hinchiranan N (2017) J Mater Res 32:788–800
17. Ayutthaya WDN, Poompradub S (2014) Macromol Res 22:686–692
18. Ostafinska A, Fortelny I, Nevoralova M, Hodan J, Kredatusova J, Slouf M (2015) RSC Adv 5:98971–98982
19. Kelnar I, Kratochvíl J, Kaprálková L (2016) J Therm Anal Calorim 124:799–805
20. Felfel RM, Leander P, Miquel G-F, Tobias M, Gerhard H, Ifty A, Colin S, Virginie S, David MG, Klaus L (2016) Biomed Mater 11:015011
21. Chee WK, Ibrahim NA, Zainuddin N, Abd Rahman MF, Chieng BW (2013) Adv Mater Sci Eng 2013:8
22. Luyt AS, Gasmi S (2016) J Mater Sci 51:4670–4681

23. Pongprayoon T, Yooprasert N, Suwanmala P, Hemvichian K (2012) Radiat Phys Chem 81:541–546
24. Bunsomsit K, Magaraphan R, O'Rear E, Grady B (2002) Colloid Polym Sci 280:509–516
25. Li WU, Zhang YE, Wu D, Li Z, Zhang H, Dong L, Sun S, Deng Y, Zhang H (2015) Adv Polym Tech 1:1–11. doi:10.1002/adv.21632
26. Janata M, Masař B, Toman L, Vlček P, Látalová P, Brus J, Holler P (2003) React Funct Polym 57:137–146
27. Jenkins MJ, Harrison KL (2006) Polym Adv Technol 17:474–478
28. Balakrishnan H, Hassan A, Wahit MU, Yussuf AA, Razak SBA (2010) M Mater Des 31:3289–3298
29. Tsuji H (2005) Macromol Biosci 5:569–597
30. Pan P, Zhu B, Kai W, Serizawa S, Iji M, Inoue Y (2007) J Appl Polym Sci 105:1511–1520
31. Zhang C, Wang W, Huang Y, Pan Y, Jiang L, Dan Y, Luo Y, Peng Z (2013) Mater Des 45:198–205
32. Fukushima K, Tabuani D, Camino G (2009) Mater Sci Eng C 29:1433–1441
33. Oksman K, Skrifvars M, Selin JF (2003) Compos Sci Technol 63:1317–1324
34. Hassouna F, Raquez J-M, Addiego F, Dubois P, Toniazzo V, Ruch D (2011) Eur Polym J 47:2134–2144
35. Liu X, Dever M, Fair N, Benson RS (1997) J Environ Polym Degr 5:225–235
36. Jeerupun J, Wootthikanokkhan J, Phinyocheep P (2004) Macromol Symp 216:281–292
37. Phinyocheep P, Saelao J, Buzaré JY (2007) Polymer 48:5702–5712
38. Kilwon C, JaeHo Y, Chan Eon P (1998) Polymer 39:3073–3081
39. Matta AK, Rao RU, Suman KNS, Rambabu V (2014) Proc Mater Sci 6:1266–1270
40. Wang Y, Xu C, Chen Z, Chen Y (2014) Polym Test 39:53–60
41. Zhao Q, Ding Y, Yang B, Ning N, Fu Q (2013) Polym Test 32:299–305
42. Hadal R, Yuan Q, Jog JP, Misra RDK (2006) Mater Sci Eng A 418:268–281
43. Ma P, Hristova-Bogaerds DG, Goossens JGP, Spoelstra AB, Zhang Y, Lemstra PJ (2012) Eur Polym J 48:146–154
44. Fu J-F, Shi L-Y, Yuan S, Zhong Q-D, Zhang D-S, Chen Y, Wu J (2008) Polym Adv Technol 19:1597–1607